Showcasing research from Dr Busupalli Balanagulu's laboratory, Department of Chemistry, School of Technology, Pandit Deendayal Energy University, Gujarat, India.

Dark-induced vertical growth of chemobrionic architectures in silver-based precipitating chemical gardens

Hydrothermal vent growth, presumed a source for origin of life, occurs at the seafloor where light penetration is limited. Silver-based chemical gardens grow in the dark, which otherwise would not form in light, portraying the significance of light-restricted dynamics in non-equilibrium processes.

As featured in:

See Balanagulu Busupalli and
Vipul Kirtikumar Patel,
Chem. Commun., 2022, **58**, 4172.

rsc.li/chemcomm

Registered charity number: 207890

ChemComm

ROYAL SOCIETY OF CHEMISTRY

COMMUNICATION

View Article Online
View Journal | View Issue

Check for updates

Cite this: *Chem. Commun.*, 2022, 58, 4172

Received 15th November 2021, Accepted 3rd February 2022

DOI: 10.1039/d1cc06430d

rsc.li/chemcomm

Dark-induced vertical growth of chemobrionic architectures in silver-based precipitating chemical gardens†

Balanagulu Busupalli *‡ and Vipul Kirtikumar Patel ‡

The light sensitivity of many silver compounds has restricted the observation of silver-based chemical gardens. Here, we report for the first time, silver-based chemical gardens grown in the dark. An identical reaction kept in the light resulted in no such structures. We attribute the observation of silver-based chemobrionics to the avoidance of light.

Chemical gardens is a term often used to describe inorganic precipitates that resemble plant like growth, and these structures grow within minutes or hours of plunging metal ion salts into anionic solutions.[1–12] Though the chemical gardens are entirely composed of inorganic moieties, they have a biologically imitative look arising from their non-equilibrium architectures. The plant like or tube-like precipitation in the chemical gardens is a consequence of the diffusive translocation of ionic species upon osmotic imbalance arising in the reaction mixture. Reactant anionic and cationic species can migrate a long distance along the tubular structures, resulting in a variety of chemical garden architectures. Following the addition of metal salt seeds, such structures are often characterised by the sudden emergence of coloured long tubular particles. The recent surge of research interest in chemical garden architectures has led to a collaborative area of research known as "Chemobrionics".[13] Many experimental techniques for producing chemical garden hollow tubes have been reported, including the injection growth method.[14,15] Some of the advanced methods to prepare these architectures include microfluidic systems,[16,17] the Hele-Shaw cell[18–21] and the delivery of a salt solution under controlled hydrostatic pressure.[22] Copper, iron, nickel, zinc and calcium-based chemical garden architectures have been extensively studied and reported to date, including their applications in ammonia sensing, light emission and fuel cells *etc.*[23–26] Gold-based chemical gardens were very recently reported.[27] There is no similar report on silver-based chemical gardens as of yet. Most silver compounds are extremely light sensitive due to which silver-based chemobrionic structures are not obtainable following conventional growth conditions, *viz.* keeping the reaction vessel under daylight/natural light or under the light from light bulbs in a typical laboratory setting. It is noted that dark-driven growth in chemical gardens has not been of any specific focus yet, but, when compared with the hydrothermal vents which form on the seafloor where light penetration is limited, these dark-grown chemobrionic architectures assume prominence. For example, in the search for life on other celestial bodies such as Enceladus on its subsurface due to its hydrothermal activity on the seafloor where penetration of light is limited and where the spewing of molecules relevant to the origin of life might occur, this result presented here on the dark-induced chemical garden growth in silver-based chemobrionics could have relevant implications for plausible biochemistry on such celestial bodies.[28,29] Thus, in this report, we first describe the experiments that resulted in silver-based chemical garden-like structures. Later, we provide substantial evidence for our hypothesis of how light restricts chemical garden-like growth in silver silicate. At the end, we propose how the removal of solvent from the as-prepared silver silicate chemical gardens results in self-assembled structures. To prepare silver-based chemical gardens, we employed silver nitrate, one of the reactants that is extremely light sensitive. Under light, cessation of chemical garden-like structures in silver silicate occurred due to the influence of light on the silver nitrate reactant causing conversion of Ag^+ ions into Ag metal. In contrast, a similar reaction mixture when kept under dark conditions in a closed cabinet produced vertically grown yellow colored chemobrionic silver silicate structures evident from the camera images depicted in Fig. 1a (for experimental details, please refer to the ESI,† and for time lapse images over the course of the production of the gardens see Fig. S1, ESI†).

Optical microscopic images revealed tube-like architectures in the as-formed silver silicate chemical gardens with a diameter of about 200–400 μm (Fig. 1b and c). These tubes appear to be brittle (ESI† Fig. S2). Microstructure from the SEM images of the

---

Department of Chemistry, School of Technology, Pandit Deendayal Energy University, Gandhinagar 382426, Gujarat, India.
E-mail: busupalli.balanagulu@sot.pdpu.ac.in

† Electronic supplementary information (ESI) available. See DOI: 10.1039/d1cc06430d

‡ Equal contribution.

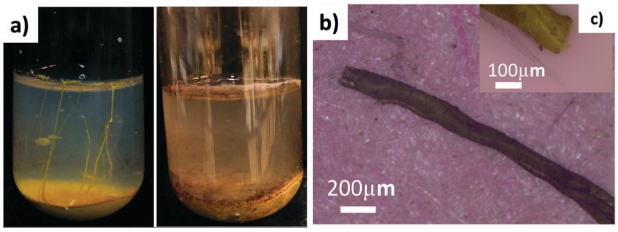

Fig. 1 (a) Camera images of the reaction vessels kept in the dark and in light. (b and c) Optical microscopic images of the as-obtained vertical structures collected from the dark reaction vessel (inset shows the tip of the tube).

as-prepared air-dried samples showed twisted tubular architectures (Fig. 2a and b). At higher magnifications, as represented in Fig. 2c and d, the surface morphology consisted of particulate matter spread across the exterior to the layers of the tubes.

To confirm our hypothesis that light hinders the growth of chemical gardens in silver-based chemobrionics, we conducted a controlled experiment in which an experimental setup was assembled (Fig. 3a). In this setup, a 632 nm red laser was employed and it was passed through a glass tube containing the silver nitrate + sodium silicate reaction mixture. The laser source was turned on continuously for 24 hours. After 24 hours, the reaction mixture yielded a white gel as the product (Fig. 3b). After noticing the white gel, we assumed that there were no vertical structures in the reaction vessel; however, when the gel was carefully segregated and discarded from the reaction vessel, some very tiny vertical tubular structures were observed in the reaction vessel grown from the bottom of the vessel. Growth of the silver silicate vertical structures, though to tiny lengths, could be accounted for by the effect of the dark conditions. But, the vertical lengths of the growth of these structures were limited because, as the laser light passed through the reaction mixture, some photons could have got diffused through the reaction mixture in all directions, which included diffusion of the photons downwards too through the reaction mixture that could have led to the sensing of these laser photons by the vertically growing structures leading to the restriction of the growth of these vertical structures to a certain vertical position in the reaction vessel (Fig. 3c). Fig. 3d shows that the experimental setup is completely closed to induce dark conditions for the reaction to occur. In the experimental setup, the cardboard box was cut to a specific width through which the laser beam could be passed onto the reaction vessel, and the rest of the box was closed (Fig. 3e). This controlled experiment using laser light actually proves that the silver based chemical gardens could not be grown under light, rather these can be grown under dark conditions. It also proves that even a few photons that got diffused from the monochromatic laser light into the reaction mixture will lead to the termination of the vertical growth in these structures.

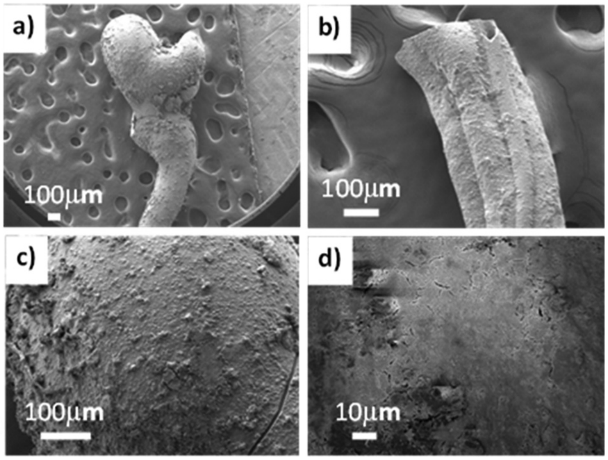

Fig. 2 SEM images of the air-dried samples. (a and b) A holistic view of the vertically grown structures, and (c and d) higher magnification images showing the microstructure.

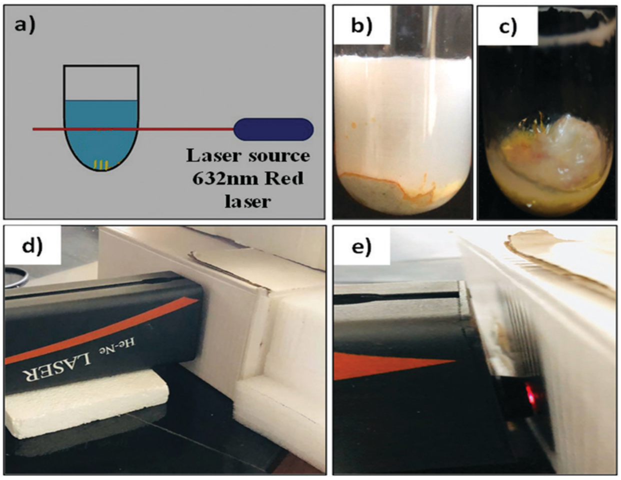

Fig. 3 (a) Cartoon representation of the setup used for the LASER experiment. (b) Gel formation. (c) Tiny vertically grown structures. (d and e) Photographs of the actual experimental setup.

In addition, we conducted a few other experiments by utilizing newly purchased silver nitrate and aged silver nitrate from other chemical manufacturers. No prominent free-standing vertical structures were observed in these cases too when the reactions were performed in light, and fully grown free-standing vertical structures were seen when the reactions were carried out under dark conditions (ESI† Fig. S3 and S4). Though the SEM imaging disclosed tubular morphology in the as-grown silver silicate chemical gardens, and *via* optical microscopic images it was evident that the structures had twisted tubular architectures, yet careful observation at the nanometre scale of these structures showed no orderly arrangement (Fig. 4a and b). Intrigued by this incongruity of arrangement from the nanoscale to the microscale, we conducted post-synthetic modification of the silver silicate chemical gardens. This was carried out by simply heating the as-prepared material in an oven at 108 °C for about 10 minutes. The oven-dried samples were then collected carefully and characterization of the same was performed. The hypothesis behind this post-synthetic modification is that the oven-drying leads to loss of any solvent/water molecules from the as-grown structure and this could give rise to

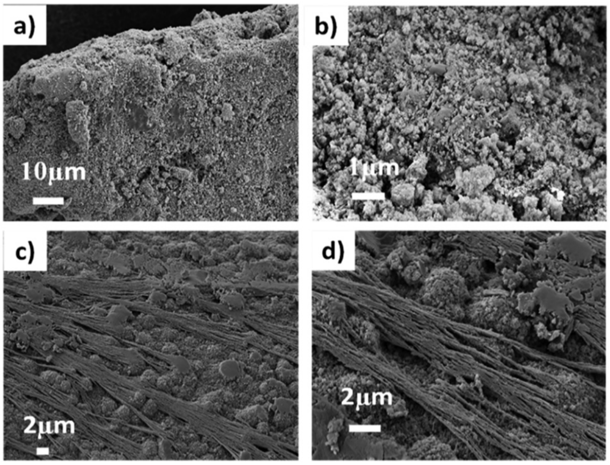

Fig. 4 SEM images of the air-dried (a and b) and oven-dried (dried at 108 °C) samples (c and d).

ordered assemblies. Fig. 4c and d show the morphological features of the oven-dried samples in SEM. Several thread-like structures were observed to form ordered assemblies emanating from globule like structures. The diameter of each thread is about 200 nm. In most cases, packs of threads constituting around 10–15 threads were observed to exist after oven-drying of the material.

Similarly, a comparison of the air-dried and oven-dried samples was performed *via* powder XRD characterization. The XRD patterns of the as-prepared air-dried silver silicate chemical garden and oven-dried sample are shown in Fig. 5. In Fig. 5, * indicates silver silicate indexing, while ■ indicates metallic silver indexing. Firstly, it is very much evident from these XRD traces that the silica amorphous halo observed in the air-dried sample is lost in the oven-dried sample indicating the collapse of any silica structures due to the loss of solvent. The broad peak from 20° to 25° shows the amorphous nature of the silica preserved in the chemical garden structures of the vertically grown air-dried silver silicate chemobrionic architectures, and this is absent in the oven-dried sample.[30] Moreover, the peaks at 33.351 and 33.824 for the air-dried sample are assigned to diffractions from the (-124) and (-115) planes of monoclinic silver silicate (JCPDS 01-085-0281), respectively.[31,32] Similarly, in the oven-dried sample, the sharp peak at 34.111 is attributed to diffraction from the (-132) plane of monoclinic silver silicate (JCPDS 01-085-0281).[31] Also, peaks at 19.11 and 32.27 for both the air-dried and oven-dried samples are assigned to diffractions from the (-111) and (033) planes of monoclinic silver silicate (JCPDS 01-085-0281). The presence of metallic silver was also observed in both the air-dried and oven-dried samples, though less intense *via* reflections at (111), (200) and (220) in the XRD with the corresponding 2θ values at 38.26°, 42.78° and 62.31° for the metallic silver in the air-dried sample and 2θ values at 38.18°, 44.25°, 64.72°, and 77.40° corresponding to the reflections (111), (200), (220), and (311) of the crystallographic planes of the face-centered cubic silver crystals in the oven-dried sample.[33,34] The XRD data thus indicate the co-presence of silver silicate and metallic silver in both the air-dried and oven-dried samples (XRD data presented after baseline correction in ESI† Fig. S5).

To confirm whether the drastic morphological differences observed from air-dried to oven-dried samples are due to changes at the molecular level in these chemical gardens, FTIR analysis was carried out at room temperature in the range of 400–4000 cm^{-1} with a scan rate of 4 cm^{-1} s^{-1}. Fig. 6 depicts the FTIR spectra comparison between the air-dried and oven-dried samples. The labelled reflections in Fig. 6 show bands at around 1042 cm^{-1} and 1383 cm^{-1} for both the oven-dried sample and the air-dried sample. At 1042 cm^{-1}, there is a strong asymmetric stretching vibration of Si–O–Si for the oven-dried and air-dried samples. Also, the reflection at 801 cm^{-1} indicates in-plane bending vibrations of Si–O geminal groups that could be due to Ag@SiO$_2$ owing to the formation of metallic silver from the decomposition of the silver silicate.[35] The rest of the bands in the two traces pertaining to the air-dried and oven-dried samples also indicate similarity in the positions of the reflections. Results from the FTIR spectra suggest that there are no noticeable changes at the molecular

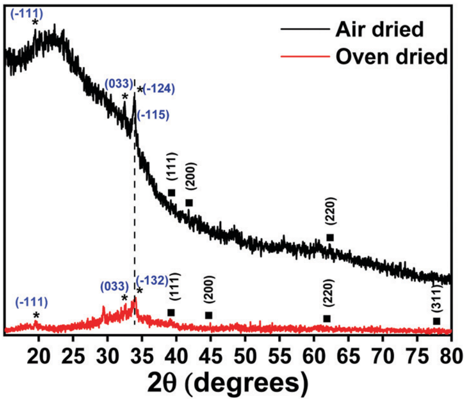

Fig. 5 PXRD patterns of the vertically grown silver silicate chemical garden after air-drying for more than 7 days and oven-drying at 108 °C for 10 minutes (upper trace for air-dried and lower trace for oven-dried; both air-drying and oven-drying were carried out in the light and not in the dark).

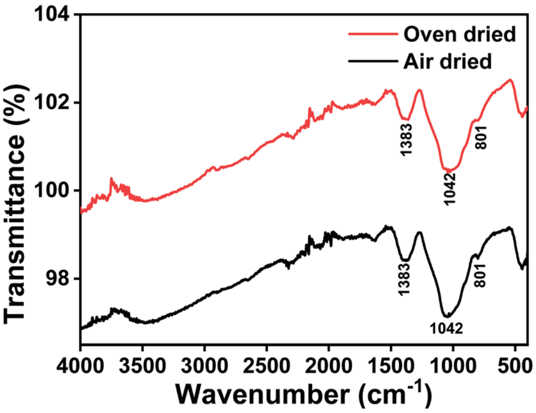

Fig. 6 FTIR of the silver silicate chemical garden. The upper trace is from the oven-dried sample and the lower trace is from the air-dried sample.

scale, and the morphological changes from air-dried to oven-dried are independent of the molecular interactions in these chemical gardens. Raman spectral analysis of both the air-dried and oven-dried samples too revealed no remarkable molecular alterations between these two samples (ESI† Fig. S6).

Following the pendency of synthesis of silver-based chemical gardens, we reported here for the first time the formation and growth of silver silicate chemical gardens. Specifically, we demonstrated here the formation of a silver silicate chemical garden in dark conditions, as well as proved with evidence that light hinders the growth of the silver-based chemical garden-like structures by performing a controlled light experiment *via* employing a red laser of wavelength 632 nm. These silver-based chemobrionic architectures were thoroughly characterized *via* optical microscopy, SEM imaging, powder XRD, FTIR spectra, digital photography and Raman spectra. Owing to the relevancy to biological structures, the dark grown silver silicate chemobrionic architectures could be of immense help to understand the role of dark conditions in some non-equilibrium processes. As this is the first report on any dark grown chemical garden, we believe this could open up a different line of study on the effect of dark conditions in chemobrionic systems.

Balanagulu Busupalli conceived the idea and directed the project. Vipul Kirtikumar Patel performed the experiments and collected the data. Both the authors analysed the data and wrote the paper.

We acknowledge PDEU-SRDC for recording FE-SEM and Raman spectra, Chemistry Department for FTIR, Mechanical Engineering Department for optical microscope, Physics Department for LASER source, and CSMCRI Bhavnagar for recording Powder XRD. BB acknowledges funding from PDEU Milestone Grant.

Conflicts of interest

The authors declare no conflicts of interest.

Notes and references

1 J. H. E. Cartwright, B. Escribano, S. Khokhlov and C. I. Sainz-Díaz, *Phys. Chem. Chem. Phys.*, 2011, **13**, 1030–1036.
2 F. Glaab, J. Rieder, J. M. García-Ruiz, W. Kunz and M. Kellermeier, *Phys. Chem. Chem. Phys.*, 2016, **18**, 24850–24858.
3 E. A. B. Hughes, T. E. Robinson, R. J. A. Moakes, M. Chipara and L. M. Grover, *Commun. Chem.*, 2021, **4**(145), 1–8.
4 S. S. S. Cardoso, J. H. E. Cartwright, J. Čejková, L. Cronin, A. De Wit, S. Giannerini, D. Horváth, A. Rodrigues, M. J. Russell, C. I. Sainz-Díaz and Á. Tóth, *Artif. Life*, 2020, **26**, 315–326.
5 S. S. S. Cardoso, J. H. E. Cartwright, O. Steinbock, D. A. Stone and N. L. Thomas, *Struct. Chem.*, 2017, **28**, 33–37.
6 F. Brau, F. Haudin, S. Thouvenel-Romans, A. De Wit, O. Steinbock, S. S. S. Cardoso and J. H. E. Cartwright, *Phys. Chem. Chem. Phys.*, 2018, **20**, 784–793.
7 E. Rauscher, G. Schuszter, B. Bohner, Á. Tóth and D. Horváth, *Phys. Chem. Chem. Phys.*, 2018, **20**, 5766–5770.
8 M. R. Bentley, B. C. Batista and O. Steinbock, *J. Phys. Chem. A*, 2016, **120**, 4294–4301.
9 C. Pimentel, J. H. E. Cartwright and C. I. Sainz-Díaz, *ChemSystemsChem*, 2020, **2**(6), e2000023.
10 E. Nakouzi and O. Steinbock, *Sci. Adv.*, 2016, **2**(8), e1601144.
11 C. I. Sainz-Díaz, B. Escribano, I. Sánchez-Almazo and J. H. E. Cartwright, *Geophys. Res. Lett.*, 2021, **48**, 1–10.
12 E. A. B. Hughes, O. Jones-Salkey, P. Forey, M. Chipara and L. M. Grover, *ChemSystemsChem*, 2021, **3**(4), e2000062.
13 L. M. Barge, S. S. S. Cardoso, J. H. E. Cartwright, G. J. T. Cooper, L. Cronin, A. De Wit, I. J. Doloboff, B. Escribano, R. E. Goldstein, F. Haudin, D. E. H. Jones, A. L. Mackay, J. Maselko, J. J. Pagano, J. Pantaleone, M. J. Russell, C. I. Sainz-Díaz, O. Steinbock, D. A. Stone, Y. Tanimoto and N. L. Thomas, *Chem. Rev.*, 2015, **115**, 8652–8703.
14 B. C. Batista, P. Cruz and O. Steinbock, *Langmuir*, 2014, **30**, 9123–9129.
15 S. Thouvenel-Romans and O. Steinbock, *J. Am. Chem. Soc.*, 2003, **125**, 4338–4341.
16 Q. Wang and O. Steinbock, *Langmuir*, 2021, **37**, 2485–2493.
17 Y. Ding, B. Batista, O. Steinbock, J. H. E. Cartwright and S. S. S. Cardoso, *Proc. Natl. Acad. Sci. U. S. A.*, 2016, **113**, 9182–9186.
18 F. Haudin, J. H. E. Cartwright, F. Brau and A. De Wit, *Proc. Natl. Acad. Sci. U. S. A.*, 2014, **111**, 17363–17367.
19 W. Zhao and K. Sakurai, *ACS Omega*, 2017, **2**, 4363–4369.
20 Q. Wang, F. M. Zanotto and O. Steinbock, *J. Phys. Chem. C*, 2020, **124**, 21617–21624.
21 L. A. M. Rocha, J. H. E. Cartwright and S. S. S. Cardoso, *Phys. Chem. Chem. Phys.*, 2021, **23**, 5222–5235.
22 B. C. Batista and O. Steinbock, *J. Phys. Chem. C*, 2015, **119**, 27045–27052.
23 M. R. Hooks, P. Webster, J. M. Weber, S. Perl and L. M. Barge, *Langmuir*, 2020, **36**, 5793–5801.
24 E. Castellini, F. Bernini, L. Sebastianelli, B. Bighi, C. Ignacio Sainz-Díaz, A. Mucci, D. Malferrari, A. Ranieri, G. Gorni, C. Marini, M. Franca Brigatti and M. Borsari, *ChemSystemsChem*, 2021, **3**, e2100034.
25 F. B. Alp, M. Gonen, S. Savrik and D. Balkose, *J. Boron.*, 2021, **6**, 227–235.
26 L. M. Barge, Y. Abedian, M. J. Russell, I. J. Doloboff, J. H. E. Cartwright, R. D. Kidd and I. Kanik, *Angew. Chem., Int. Ed.*, 2015, **54**, 8184–8187.
27 G. D. Zissi, G. Angelis and G. Pampalakis, *ChemSystemsChem*, 2021, **3**, e2000018.
28 G. Angelis, G. G. Kordopati, E. Zingkou, A. Karioti, G. Sotiropoulou and G. Pampalakis, *Chem. – Eur. J.*, 2021, **27**, 600–604.
29 S. S. S. Cardoso, J. H. E. Cartwright and C. I. Sain-Díazz-Díaz, *Icarus*, 2019, **319**, 337–348.
30 L. Y. Yu, Z. X. Huang and M. X. Shi, *Adv. Mater. Res.*, 2014, **1030–1032**, 189–192.
31 R. Cao, H. Yang, X. Deng, S. Zhang and X. Xu, *Sci. Rep.*, 2017, **7**, 1–12.
32 J. Liu, W. Wu, Q. Tian, Z. Dai, Z. Wu, X. Xiao and C. Jiang, *Dalton Trans.*, 2016, **45**, 12745–12755.
33 D. Acharya and B. Mohanta, *AIP Conf. Proc.*, 2017, **1832**, 050155.
34 K. Shameli, M. Bin Ahmad, A. Zamanian, P. Sangpour, P. Shabanzadeh, Y. Abdollahi and M. Zargar, *Int. J. Nanomed.*, 2012, **7**, 5603–5610.
35 I. Ramalla, R. K. Gupta and K. Bansal, *Int. J. Eng. Technol.*, 2015, **4**, 509.